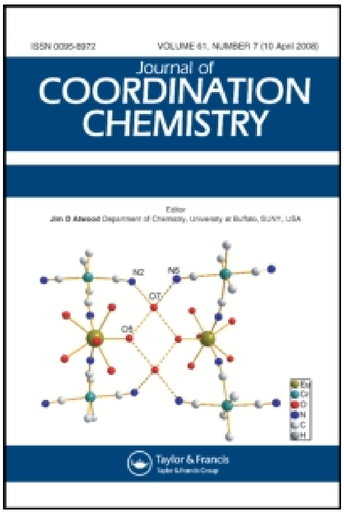

Journal of Coordination Chemistry
Publication details, including instructions for authors and subscription information:
http://www.informaworld.com/smpp/title~content=t713455674

Electrocatalytic reduction of molecular oxygen at electrodes coated with a new cobalt(II)-platinum(II) bimetallic porphyrin

Shawn Swavey[a]; Muralikrishna Narra[a]; Habib Srour[a]
[a] Department of Chemistry, University of Dayton, Dayton, OH. 45469-2357, USA

To cite this Article Swavey, Shawn , Narra, Muralikrishna and Srour, Habib(2005) 'Electrocatalytic reduction of molecular oxygen at electrodes coated with a new cobalt(II)-platinum(II) bimetallic porphyrin', Journal of Coordination Chemistry, 58: 16, 1463 — 1476

To link to this Article: DOI: 10.1080/00958970500230301

URL: http://dx.doi.org/10.1080/00958970500230301

Journal of Coordination Chemistry
Vol. 58, No. 16, 10 November 2005, 1463–1476

Taylor & Francis
Taylor & Francis Group

Electrocatalytic reduction of molecular oxygen at electrodes coated with a new cobalt(II)–platinum(II) bimetallic porphyrin

SHAWN SWAVEY*, MURALIKRISHNA NARRA and HABIB SROUR

Department of Chemistry, University of Dayton, 300 College Park,
Dayton, OH. 45469-2357, USA

(*Received in final form 21 June 2005*)

Cobalt(II) inserts into 5-(4-pyridyl)-10,15,20-(3,4-dimethoxyphenyl)porphyrin (**1**) by reaction of the porphyrin with the cobalt(II) acetate salt in refluxing *N*,*N*′-dimethylformamide solutions. When the porphyrin and the cobalt porphyrin are reacted with $PtCl_2(DMSO)_2$ in dichloromethane at ambient temperatures the platinum complex coordinates to the peripheral pyridyl group of the porphyrin. Roughened EPG electrodes coated with the cobalt(II)–platinum(II) bimetallic porphyrin, complex (**4**), show a 500 mV shift in the reduction of molecular oxygen in acidic media when compared to the bare electrode. Oxidation of the bimetallic porphyrin coated electrodes at 1.20 V *versus* saturated calomel electrode (SCE) results in an additional shift of ca 100 mV for the reduction of molecular oxygen when compared to the bimetallic porphyrin coated electrode prior to oxidation. In addition the oxidized surface shows the ability to reduce approximately 50% of the oxygen to water and the other 50% to hydrogen peroxide according to rotating disk electrode measurements.

Keywords: Porphyrin; Oxygen reduction; Cobalt(II); Platinum(II); Electrode adsorption

1. Introduction

Macrocyclic complexes have been extensively studied as electrocatalysts in fuel cell applications [1–4]. An ideal electrocatalyst for fuel cell applications should reduce oxygen by four electrons directly to water at a potential near the thermodynamically allowed value and avoid formation of potentially destructive intermediates such as superoxide or hydrogen peroxide. Within the class of macrocyclic complexes, cobalt and iridium metalloporphyrins have shown the most promise for the electrocatalytic reduction of oxygen [5, 6]. Cobalt(II) porphyrins are known to reduce oxygen at the most positive potentials, however, in most cases this reduction is by two electrons to form hydrogen peroxide.

---

*Corresponding author. Email: shawn.swavey@notes.udayton.edu

Journal of Coordination Chemistry
ISSN 0095-8972 print: ISSN 1029-0389 online © 2005 Taylor & Francis
DOI: 10.1080/00958970500230301

Some ingenious complexes have been synthesized in the hopes of converting cobalt(II) porphyrins into electrocatalysts capable of reducing oxygen directly to water at high positive potentials. Cofacial dicobalt porphyrins, for example, have been shown to catalyze the reduction of oxygen to water through direct interaction of both metal centers with the two oxygen atoms of O_2 [7–9]. However, few examples exist in which a monomeric cobalt porphyrin catalyzes the four electron reduction of oxygen. In a series of studies it was shown that by coordination of three or four substitutionally inert $Ru(II)(NH_3)_5$ moieties to the meso-pyridyl nitrogens of cobalt(II) tetra-(4-pyridyl)porphyrin, adsorbed onto pyrolytic graphite electrodes, the direct four-electron reduction of oxygen to water at catalytic potentials could be achieved [10]. It was initially thought that the peripheral Ru(II) redox centers donated electrons to the Co(II) metal center leading to the reduction of O_2 directly to H_2O. Subsequent studies revealed that the multi-electron reduction of O_2 to H_2O with these complexes is the result of increased electron density placed on Co(II) through π-backbonding of the pyridyl groups with the Ru(II) groups. Electrodes coated with monomeric multimetallic porphyrins of this type were found to be unstable in acidic media [10].

Stability of many electrocatalysts has been improved by their incorporation into polymer films and through electropolymerization of the catalysts directly onto electrode surfaces [11–14]. Numerous studies on the electropolymerization of porphyrins onto electrode surfaces showed formation of thin conductive films for use in electrocatalysis [15], biosensors [16] and electroanalysis [17]. Synthetically incorporating electroactive organic pendant groups into the porphyrin framework and utilizing the ability of these groups to undergo either electro-oxidation or electro-reduction has led to the formation of polymeric arrays on the electrode surface. Electrodes modified in this manner act both as the medium and the mediator for electron-transfer and have been used to catalyze the reactions of small molecules [18–20].

This article describes the synthesis and characterization of cobalt(II), platinum(II) and cobalt(II)–platinum(II) complexes of 5-(4-pyridyl)-10,15,20-(3,4-dimethoxyphenyl) porphyrin (**1**). When adsorbed onto edge plane pyrolytic graphite (EPG) electrodes and cycled anodically in acidic media these complexes undergo an oxidative process. The effect of this oxidative process on the ability of the coated electrodes to catalyze the reduction of oxygen is presented.

2. Experimental

2.1. *General*

All reagents were analytical grade unless stated otherwise. 4-Pyridine-carboxaldehyde, 3,4-dimethoxybenzaldehyde, propionic acid, cobalt(II) acetate, methanol, acetonitrile, methylene chloride, perchloric acid, *N*,*N*′-dimethylformamide (DMF), (60–200 mesh) silica gel, tetrabutyl ammonium hexafluorophosphate, Bu_4NPF_6 (TBAP), used as supporting electrolyte for electrochemistry, and spectroquality acetonitrile (for electrochemistry) were used without further purification. 5-(4-Pyridyl)-10,15,20-triphenylporphyrin (**5**) [21], *cis*-$Pt(DMSO)_2Cl_2$ [22], H_2MPyTPP-Pt (**6**) [23] and 5-(4-pyridyl)-10,15,20-(3,4-dimethoxyphenyl)porphyrin (**1**) [24] were prepared according to literature procedures. Pyrrole was vacuum distilled prior to use. Elemental analyses were performed by Atlantic Microlab, Norcross, GA.

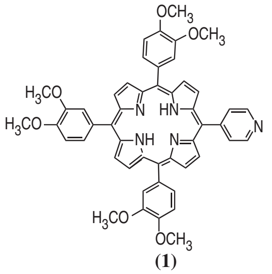
(1)

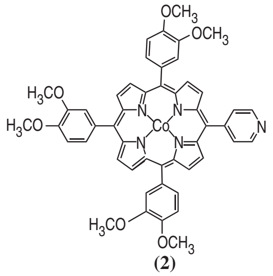
(2)

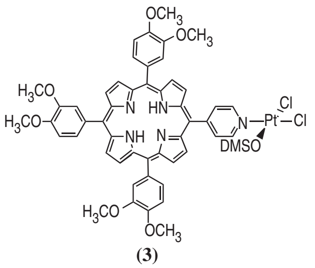
(3)

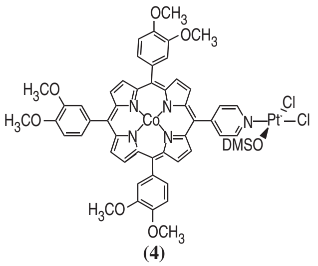
(4)

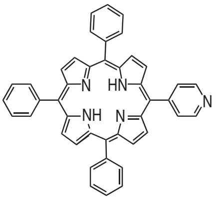
(5)

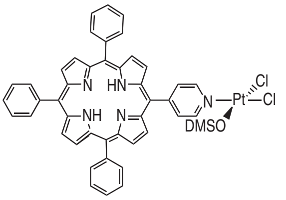
(6)

UV-Vis spectra were recorded at room temperature using a Schimadzu 1501 photodiode array spectrophotometer with 2 nm resolution. Samples were run in UV-grade CH_2Cl_2 in 1 cm quartz cuvettes. ^{1}H NMR spectra were recorded on a Bruker 300 MHz spectrometer using $CDCl_3$ as the solvent and tetramethylsilane (TMS) as the internal standard. Solution cyclic voltammograms were recorded using a one-compartment, three electrode cell, CH-Instruments, equipped with a platinum wire auxiliary electrode. The working electrode was a 2.0 mm diameter platinum disk from CH-Instruments. The working electrode was polished first using 0.30 μ followed by 0.05 μ alumina polish (Buehler) and then sonicated for 20 s prior to use. Potentials were referenced to a saturated calomel electrode (SCE). The supporting electrolyte was 0.1 M TBAP and the measurements were made in DMF.

2.2. *Electrode preparation*

Adsorption of the porphyrins and metallo-porphyrins onto an EPG electrode (AFE3T 5.0 mm diameter, Pine Instrument Co.) which had been roughened using 400 grit sandpaper was accomplished by placing 20 μL aliquots of 0.005 to 0.010 mM acetone or dichloromethane solutions of the porphyrins onto the electrode surface and allowing the solvent to evaporate at 20°C. The electrodes were then washed with distilled water and tapped dry with a kimwipe. Cyclic voltammetry and rotating disk electrode (RDE) experiments of the modified electrodes were performed using a Pine AFCBP1 bipotentiostat and an AFMSRX rotator (Pine Instrument Co.) in 0.50 M perchloric acid solutions that were 0.25 M in ammonium hexafluorophosphate (NH_4PF_6).

2.3. *Preparations*

2.3.1. 5-(4-pyridyl)-10,15,20-(3,4-dimethoxyphenyl)porphyrin (1). UV-Vis (CH_2Cl_2) λ_{max} (nm) [$\varepsilon \times 10^{-4}$ ($M^{-1}cm^{-1}$)]: 423 [22.8], 518 [1.28], 555 [0.74], 592 [0.47], 649 [0.39]. ^{1}H NMR (300 MHz, $CDCl_3$, TMS): δ 9.03 (2H, d, 2,6-pyridyl), 8.94 (6H, m, pyrrole *β*), 8.79 (2H, d, pyrrole *β*), 8.17 (2H, d, 3,5-pyridyl), 7.76 (6H, m, 2{3,4-dimethoxyphenyl} and 6{3,4-dimethoxyphenyl}), 7.26 (3H, d, 5{3,4-dimethoxyphenyl}), 4.18 (9H, s, *p*-methoxy), 3.99 (9H, s, *m*-methoxy), −2.78 (2H, s, internal pyrrole). [$C_{49}H_{41}N_5O_6 \cdot 2H_2O$] Anal. Calcd (%): C, 70.74; H, 5.45; N, 8.42. Found: C, 70.41; H, 5.27; N, 7.92.

2.3.2. 5-(4-pyridyl)-10,15,20-(3,4-dimethoxyphenyl)porphyrinatocobalt(II) (2). To a solution of 200 mg (0.250 mmol) of **1** in DMF was added 75 mg of cobalt(II) acetate and the solution was refluxed under nitrogen for 30 min. The solution was allowed to cool to room temperature and poured into 20 mL of distilled water. The reddish-brown precipitate was filtered and washed 2 × 10 mL with cold distilled water followed by 2 × 5 mL of cold absolute ethanol and finally 2 × 15 mL diethyl ether (120 mg, 0.140 mmol, 57% yield). UV-vis (CH_2Cl_2) λ_{max} (nm) [$\varepsilon \times 10^{-4}$ ($M^{-1}\,cm^{-1}$): 416 [15.6], 530 [1.27]. [$C_{49}H_{39}N_5O_6Co \cdot H_2O$] Anal. Calcd (%): C, 67.58; H, 4.75; N, 8.04. Found: C, 67.48; H, 4.64; N, 7.80.

2.3.3. *cis*-Pt(DMSO)[MPy3, 4DMPP)H$_2$]Cl$_2$ (3). To a solution containing 80 mg (0.10 mmol) of **1** in 20 mL of dichloromethane was added 42 mg (0.10 mmol) of *cis*-Pt(DMSO)$_2$Cl$_2$ and the solution was stirred at ambient temperature for 4 h. The solvent was removed and the resulting violet powder was chromatographed on silica gel using a 50 : 50 ethyl acetate/chloroform mixture as the eluent. The first red band off the column was collected and the solvent removed under reduced pressure (61 mg, 0.053 mmol, 53% yield). UV-Vis (CH_2Cl_2) λ_{max} (nm) [$\varepsilon \times 10^{-4}$ ($M^{-1}\,cm^{-1}$)]: 426 [37.2], 520 [1.63], 558 [1.06], 593 [0.61], 651 [0.57]. ^1H NMR (300 MHz, $CDCl_3$, TMS): δ 9.19 (2H, d, 2,6-pyridyl), 9.00 (2H, d, pyrrole *β*), 8.93 (4H, s, pyrrole *β*), 8.76 (2H, d, pyrrole *β*), 8.29 (2H, d, 3,5-pyridyl), 7.76 (6H, m, 2{3,4-dimethoxyphenyl} and 6{3,4-dimethoxyphenyl}), 7.29 (3H, d, 5{3,4-dimethoxyphenyl}), 4.19 (9H, s, *p*-methoxy), 4.00 (9H, s, *m*-methoxy), 3.62 (6H, s, DMSO), −2.77 (2H, s, internal pyrrole). [$C_{51}H_{47}N_5O_7Cl_2SPt \cdot H_2O$] Anal. Calcd (%): C, 52.90; H, 4.26; N, 6.05. Found: C, 52.78; H, 4.26; N, 6.05.

2.3.4. *cis*-Pt(DMSO)[MPy3, 4DMPP)Co]Cl$_2$ (4). To a solution containing 85 mg (0.10 mmol) of **2** in 20 mL of dichloromethane was added 42 mg (0.10 mmol) of *cis*-Pt(DMSO)$_2$Cl$_2$ and the solution was stirred at ambient temperature for 4 h. The solvent was removed and the resulting powder was flash precipitated by dissolving the residue in 5 mL of acetonitrile followed by dropwise addition to 250 mL of diethyl ether to give a black microcrystalline powder (62 mg, 0.052 mmoles, 52% yield). UV-Vis (CH_2Cl_2) λ_{max} (nm) [$\varepsilon \times 10^{-4}$ ($M^{-1}\,cm^{-1}$)]: 419 [18.2], 532 [1.53]. [$C_{51}H_{45}N_5O_7Cl_2SPtCo$] Anal. Calcd (%): C, 51.18; H, 3.79; N, 5.85. Found: C, 51.29; H, 3.76; N, 5.67.

3. Results and discussion

The synthesis of **1** has been described elsewhere [24]. Insertion of cobalt(II) into the porphyrin center was accomplished using the procedure developed by Adler *et al.* [25]. Coordination of Pt(DMSO)Cl$_2$ to the peripheral pyridyl group of **1** was adapted from the procedure used to synthesize **6** [23]. The synthesis of **1** led to six different

Table 1. Solution cyclic voltammetry (CV) and UV-Vis spectroscopy results for complexes **1**–**6**.

Complex no.	$E_{1/2}$ (V)/(ΔE_p)	λ_{max} (nm)
1	−0.99(80) −1.44 (100) $E_{pa} = 1.15$	423 (Soret) 518, 555, 592, 649 (Q-bands)
2	−0.72 (80)	416 (Soret) 530
3	−0.95 (55) $E_{pc} = -1.16$ −1.43 (130) $E_{pa} = 1.15$	426 (Soret) 520, 558, 593, 651 (Q-bands)
4	−0.71 (90)	419 (Soret) 532
5	−0.96 (70) −1.41 (100) $E_{pa} = 1.21$	418 (Soret) 514, 548, 588, 646 (Q-bands)
6	−0.89 (60) $E_{pc} = -1.15$ −1.40 (80) $E_{pa} = 1.26$	420 (Soret) 516, 552, 591, 642 (Q-bands)

Note: Cyclic voltammograms were run in 0.2 M TBAP/DMF solutions purged with N_2 and referenced to the saturated calomel electrode (SCE). Electronic spectra were taken in 1 cm quartz cells in dichloromethane.

porphyrins making it difficult to purify and identify the target molecule. ^{1}H NMR was used to help identify the porphyrin (**1**) and its Pt(II) analog. Identification of the target porphyrin was made easier by comparison of the integrated proton spectrum of the pyridyl protons with the protons associated with the methoxy substituents. This method was also utilized to identify the Pt(II) complex (**3**) by comparing the methoxy protons associated with the porphyrin to the methyl protons of the DMSO ligand substituent. The methoxy protons of complex **3** occur as singlets in the ^{1}H NMR spectrum at 4.19 ppm for the *p*-methoxy protons and 4.00 ppm for the *m*-methoxy protons. Protons associated with the methyl groups of the dimethylsulfoxide (DMSO) ligand occur as a singlet at 3.62 ppm. Integration of these protons results in a 3 : 3 : 2 ratio in agreement with the proposed structure of complex **3**. The harsh conditions needed to insert Co(II) into the porphyrin center, refluxing DMF, may cause decomposition of the peripheral Pt(DMSO)Cl_2 moiety therefore coordination of $Pt(DMSO)_2Cl_2$ was attempted on complex **2**. This route to the bimetallic complex **4** was simple and clean, leading to good product yields.

The electronic transitions associated with the complexes **1**–**4** are described in table 1. Insertion of cobalt(II) increases the symmetry of the porphyrin complex causing a collapse of the four Q-bands associated with the free-base porphyrin into one band at 530 nm. A shift in the Soret band from 423 nm for complex **1** to 416 nm for complex **2** is also observed. A slight shift in the Soret band from 423 to 426 nm is observed upon coordination of Pt(DMSO)Cl_2 to the pyridyl group of complex **1**. The Q-bands associated with complex **3** experience a similar shift to lower energy. Coordination of Pt(DMSO)Cl_2 to complex **2** also results in a shift to lower energy by 2 to 3 nm. The UV-Vis data in table 1 indicate only a slight perturbation by Pt(DMSO)Cl_2 of the orbitals responsible for the electronic transitions of the platinated porphyrins.

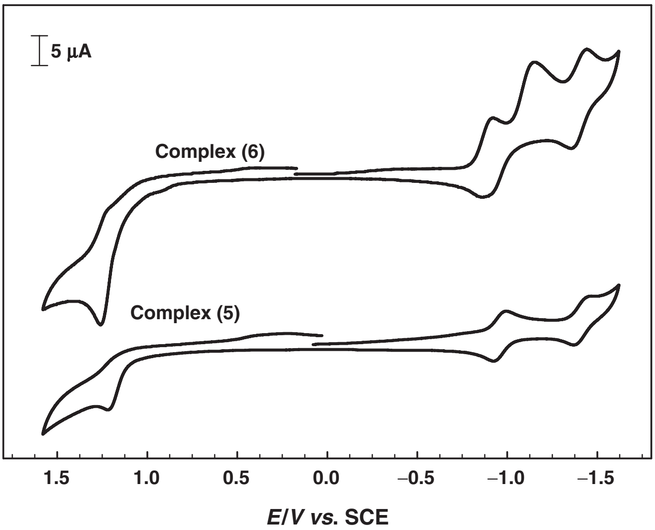

Figure 1. Solution cyclic voltammograms of millimolar solutions of complex **5**, bottom curve, and complex **6**, top curve, in 0.2 M TBAP/DMF *vs.* SCE. Working electrode is Pt with a scan rate of $100\,\mathrm{mV\,s^{-1}}$ under a nitrogen atmosphere.

Electrochemical properties of the complexes were studied in DMF solution by cyclic voltammetry (CV). Table 1 lists the redox potentials associated with the complexes. The synthesis and spectroscopic characteristics of complex **6** have been reported [23], however, no literature on the solution electrochemistry of this complex could be found. For comparative purposes the CV results for complexes **5** and **6** have been included.

The cyclic voltammograms of **5** and **6** in 0.2 M TBAP/DMF solution are illustrated in figure 1 and summarized in table 1. The cathodic region of the voltammogram for **5** shows two quasi-reversible redox couples associated with formation of the porphyrin monoanion and dianion, respectively [26]. An irreversible oxidation wave with $E_{\mathrm{pa}} = 1.21\,\mathrm{V}$ is due to formation of the porphyrin radical cation, which undergoes a chemical reaction following its formation.

The cyclic voltammogram of **6**, top curve figure 1, shows that coordination of $\mathrm{Pt(DMSO)Cl_2}$ stabilizes the π^*-orbitals of the porphyrin shifting their redox couples to less negative values, table 1. In addition the redox couples associated with **6** are more reversible than the free-base porphyrin indicating that coordination of $\mathrm{Pt(DMSO)Cl_2}$ increases the electron transfer kinetics. In the anodic direction the irreversible oxidation associated with porphyrin cation formation is shifted to more positive potentials by the Pt(II) moiety, table 1. An irreversible reduction process at $E_{\mathrm{pc}} = -1.15\,\mathrm{V}$, figure 1, is associated with the Pt(II) metal center and is tentatively assigned to the reduction of Pt(II) to Pt(I) based on voltammetric studies of square planar Pt(II) complexes in aprotic media [27, 28].

Figure 2 illustrates the redox chemistry of complex **3** and complex **1** under the same conditions as those in figure 1. Comparison of the cyclic voltammograms of figures 1 and 2 reveal many similarities between the two porphyrins and their Pt(II) analogs. Some noticeable differences, however, are clearly indicated in table 1. First the irreversible oxidation observed for complex **1**, $E_{\mathrm{pa}} = 1.15\,\mathrm{V}$, is unaffected

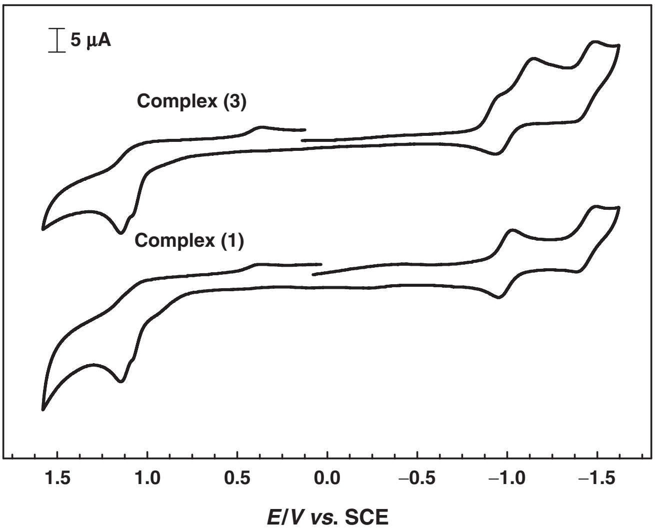

Figure 2. Solution cyclic voltammograms of millimolar solutions of complex **1**, bottom curve, and complex **3**, top curve, in 0.2 M TBAP/DMF *vs.* SCE. Working electrode is Pt with a scan rate of $100\,\mathrm{mV\,s^{-1}}$ under a nitrogen atmosphere.

by Pt(II) coordination and occurs at less positive potentials than the irreversible oxidation associated with complex **5**, $E_{\mathrm{pa}} = 1.21\,\mathrm{V}$. This suggests that the initial oxidation of **1** and **3** is localized on the π-orbitals of the peripheral 3,4-dimethoxyphenyl substituents which are easier to oxidize than the phenyl substituents on **5**. Reduction of the platinum center occurs at the same potential for both platinated porphyrins; however, the reduction potential leading to radical anion formation is less affected by Pt(II) coordination in the case of **3**, $E_{1/2} = -0.95\,\mathrm{V}$, than with **6**, $E_{1/2} = -0.89\,\mathrm{V}$. The result is the partial overlap of the cathodic waves in figure 2, top curve, and much more defined cathodic waves in figure 1.

Figure 3 shows the cyclic voltammograms for complex **2** and complex **4** in 0.2 M TBAP/DMF solutions. A quasi-reversible redox couple is observed with an $E_{1/2} = -0.72$ and $E_{1/2} = -0.71\,\mathrm{V}$ for the cobalt(II) porphyrin and the cobalt(II)/platinum(II) porphyrin, respectively. This is attributed to the Co(II/I) redox couple [29]. The Co(III/II) couple is not observed due to slow electron transfer kinetics in DMF [29]. In the anodic direction a broad irreversible oxidation process associated with cation formation is observed for both compounds.

3.1. *Electrode adsorption*

After scoring the surface of an EPG electrode, using 400 grit sandpaper, 20 μL of 10^{-5} M solutions of acetone or dichloromethane containing the desired complex were placed onto the electrode and the solvent was evaporated under ambient conditions. Reproducible surfaces were obtained in this manner as indicated by CV experiments. Electrochemical properties of the complexes adsorbed onto EPG electrodes were studied in 0.50 M $HClO_4$/0.25 M NH_4PF_6 solution by CV.

Every adsorbed complex studied by CV displayed Faradaic current when anodically cycled to 1.20 V in the acidic media. This current was in the form of an irreversible

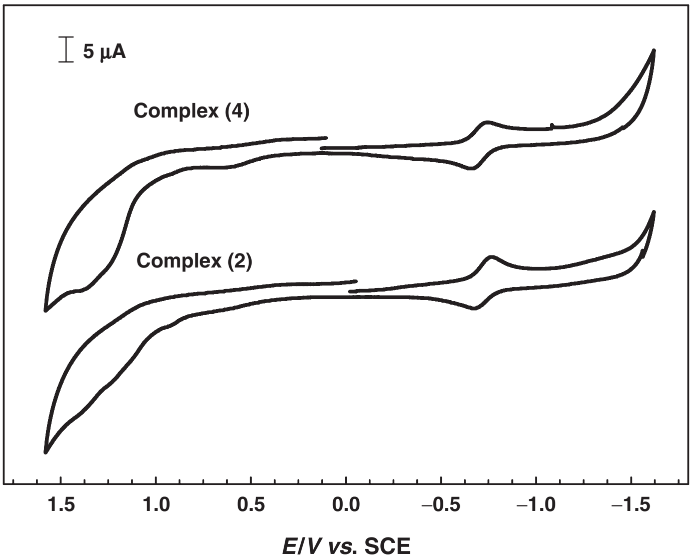

Figure 3. Solution cyclic voltammograms of millimolar solutions of complex **2**, bottom curve, and complex **4**, top curve, in 0.2 M TBAP/DMF *vs.* SCE. Working electrode is Pt with a scan rate of $100\,\mathrm{mV\,s^{-1}}$ under a nitrogen atmosphere.

Table 2. Cyclic voltammetry (CV) results for the bare EPG electrode and complexes **1**–**4** adsorbed onto an EPG electrode run in 0.50 M $HClO_4$/0.25 M NH_4PF_6 solutions. Peak potentials reported *vs.* SCE.

		Oxygen reduction	
Complex no.	E_{pa} (V)	E_{pc} (V) (before oxidation)	E_{pc} (V) (after oxidation)
EPG (bare)	–	−0.39	–
1	1.03	−0.44	−0.41
2	1.18	0.00	0.00
3	1.04 (br)	−0.44	−0.21 (br)
4	1.02 (br)	0.09	0.14

oxidation wave most likely due to formation of the radical cation associated with the porphyrin ring. Table 2 summarizes the results of this study. When complex **4** was adsorbed onto the EPG electrode and cycled anodically in 0.50 M $HClO_4$/0.25 M NH_4PF_6 an irreversible oxidation with a broad peak potential of ca 1.02 V was observed as illustrated in figure 4. Unlike the other complexes studied when the scan is reversed a new reduction wave at 0.48 V coupled to an oxidation wave at 0.55 V appears which was not present on the initial scan. This new redox couple is the result of an electrochemical–chemical–electrochemical (ECE) type mechanism. It is unclear at this point why the other porphyrin complexes do not form a new redox couple upon oxidation. The chemical reaction involved in the ECE mechanism is more than likely oxidative demethylation of the 3,4-dimethoxyphenyl groups to form a quinone complex capable of being reduced reversibly to the hydroquinone, however, this does not explain the role of Co(II) or Pt(II) in this process [30–32].

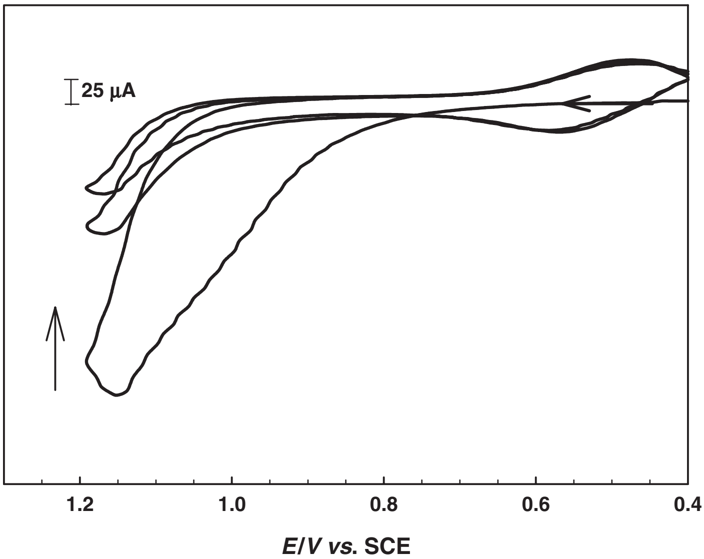

Figure 4. Cyclic voltammogram of complex **4** adsorbed onto an EPG electrode in 0.50 M $HClO_4$/0.25 M NH_4PF_6 solution *vs.* SCE. Scan rate = 100 mV s^{-1}.

3.2. *Oxygen reduction*

Oxygen reduction studies of the complexes adsorbed onto roughened EPG electrodes were accomplished by performing CV and RDE experiments in aqueous 0.50 M $HClO_4$/0.25 M NH_4PF_6 solutions saturated with air. The peak potentials for oxygen reduction at the various coated electrodes before and after cycling to 1.20 V *versus* SCE are given in table 2. Reduction of oxygen at the bare electrode occurs at $E_{pc} = -0.39$ V. EPG electrodes coated with porphyrins which do not contain a cobalt(II) metal center reduce oxygen at potentials more negative than the bare electrode. In the case of electrodes coated with complex **3**, which does not contain a cobalt metal center, a shift of over 200 mV, from −0.44 to −0.21 V, is observed for oxygen reduction after the coated electrode has been cycled to 1.20 V. Square planar Pt(II) complexes have been shown to electrocatalytically reduce oxygen in acidic solutions [33]. The need for anodic conditioning prior to the observed catalysis may be due to formation of a more ordered film on the electrode exposing the Pt(II) centers to the air saturated solution. A 400 mV catalytic shift in the reduction of oxygen when compared to the bare electrode is observed when electrodes coated with complex **2** are cycled in acidic solutions, table 2. Anodic conditioning of this electrode does not lead to enhanced catalysis as was observed for complex **3**.

The greatest catalytic shift was observed for the EPG electrode coated with complex **4**. Oxygen reduction with this electrode occurs with $E_{pc} = 0.09$ V, dotted line figure 5. After cycling the coated electrode to 1.20 V the reduction of oxygen is shifted to $E_{pc} = 0.14$ V, solid line figure 5. In addition to the 50 mV shift to more positive potentials a marked increase in current for the reduction of oxygen is observed after complex **4** is anodically conditioned onto the EPG electrode.

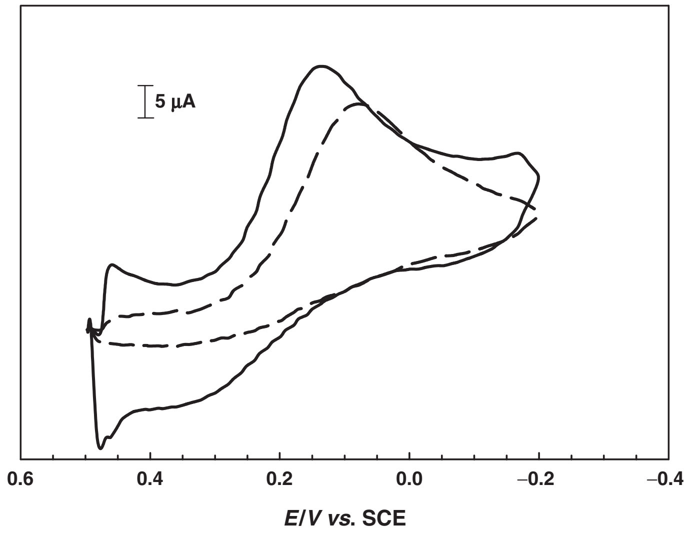

Figure 5. Cyclic voltammogram for the reduction of O_2 in 0.50 M $HClO_4$/0.25 M NH_4PF_6 on an EPG electrode coated with complex **4** before oxidation at 1.20 V, dotted line, and after oxidation at 1.20 V, solid line. Reference is SCE, scan rate = 100 mV s^{-1}.

3.3. *Rotating disk electrode (RDE) studies*

To determine the extent of the reduction process RDE experiments were performed on the coated EPG electrodes in air saturated acidic solutions. The two most likely pathways for oxygen reduction are by two electrons forming hydrogen peroxide or the direct four electron process resulting in the formation of water. RDE studies give insight into the number of electrons transferred to the analyte by comparing the plateau currents to the rotation rate of the electrode. Although electrodes coated with complex **2** display a catalytic shift in the reduction of oxygen compared to the bare electrode, the slow electrode kinetics prevent formation of a plateau current even at very negative potentials. Therefore only electrodes coated with complex **4** could be studied by RDE.

Figure 6(a) illustrates the results of the RDE experiments performed on a roughened EPG electrode coated with complex **4** in air saturated 0.50 M $HClO_4$/0.25 M NH_4PF_6 solution. A plot of the diffusion-limited current density *versus* the square root of the rotation rate, the Levich plot, is shown in figure 6(b). Deviation from linearity at the higher rotation rates is attributed to a potential independent rate limiting step, most likely the formation of the Co(II)–O_2 bond [5]. The Koutecky–Levich plot, figure 6(c), relates the plateau current density to the rotation rate using equation (1) [34]:

$$\begin{aligned}\frac{1}{I_L} &= \frac{1}{I_k} + \frac{1}{B\omega^{1/2}} \\ B &= 0.2nFCv^{-1/6}D^{2/3}\end{aligned} \tag{1}$$

where I_L is the current density (A cm^{-2}), n is the number of electrons for the reaction, F is the Faraday constant (96,500 C mol^{-1}), D is the diffusion coefficient of O_2 in the solution (2.0×10^{-5} $cm^2 s^{-1}$), v is the kinematic viscosity of the solution (0.01 $cm^2 s^{-1}$), C is the concentration of O_2 in the air-saturated solution (0.25 mM),

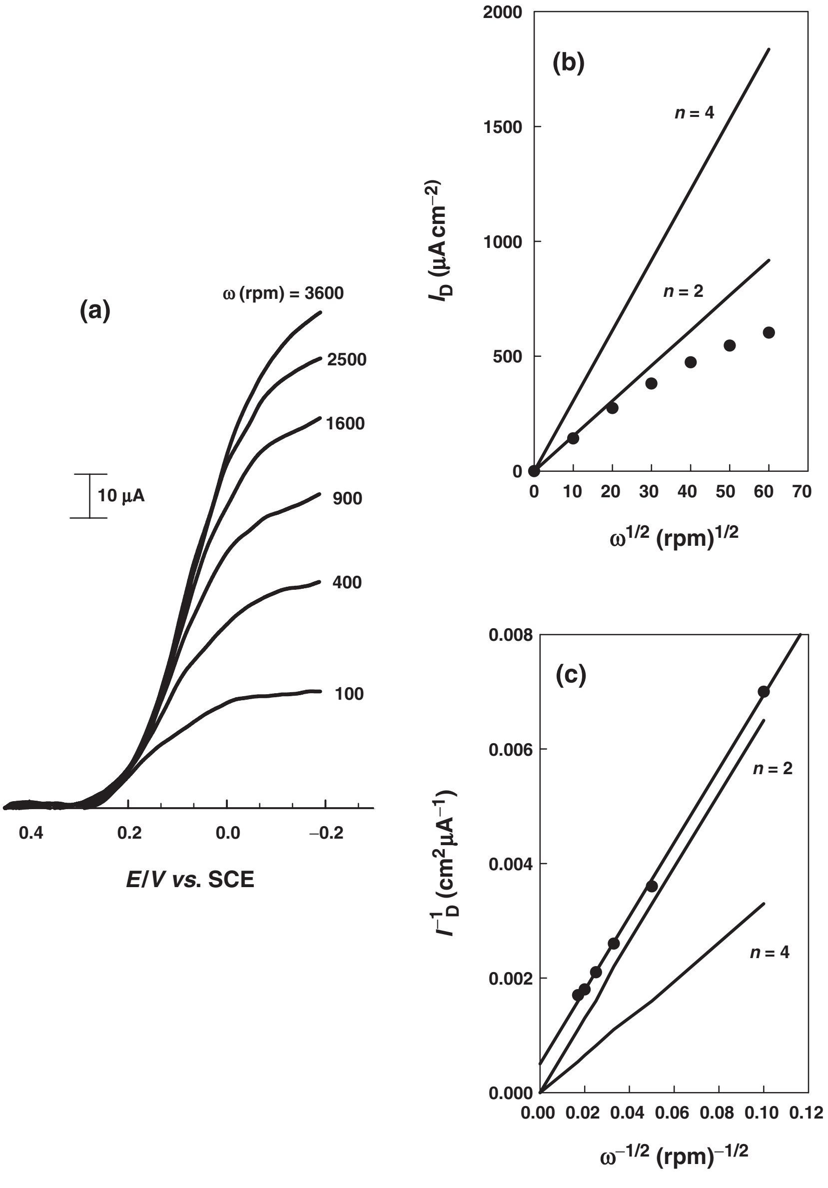

Figure 6. Reduction of O_2 at a rotating disk electrode coated with complex **4** prior to oxidation at 1.20 V. (a) Current–potential curves in air saturated 0.50 M $HClO_4$/0.25 M NH_4PF_6, scan rate = 5 mV s^{-1}. (b) Levich plot of plateau current *vs.* square root of the rotation rate for the curves in (a). (c) Koutecky–Levich plot of the inverse of the plateau current *vs.* the inverse of the square root of the rotation rate for the curves in (a). The theoretical two electron and four electron lines are marked $n = 2$ and $n = 4$, respectively.

and ω is the rotation rate (rpm). I_k is the kinetic current density for O_2 reduction and can be calculated from the intercept of the Koutecky–Levich plot. The slope of the Koutecky–Levich plot for the experimental data parallels the theoretical $n = 2$ line, figure 6(c), indicating that reduction of oxygen at this electrode is by two electrons to form hydrogen peroxide.

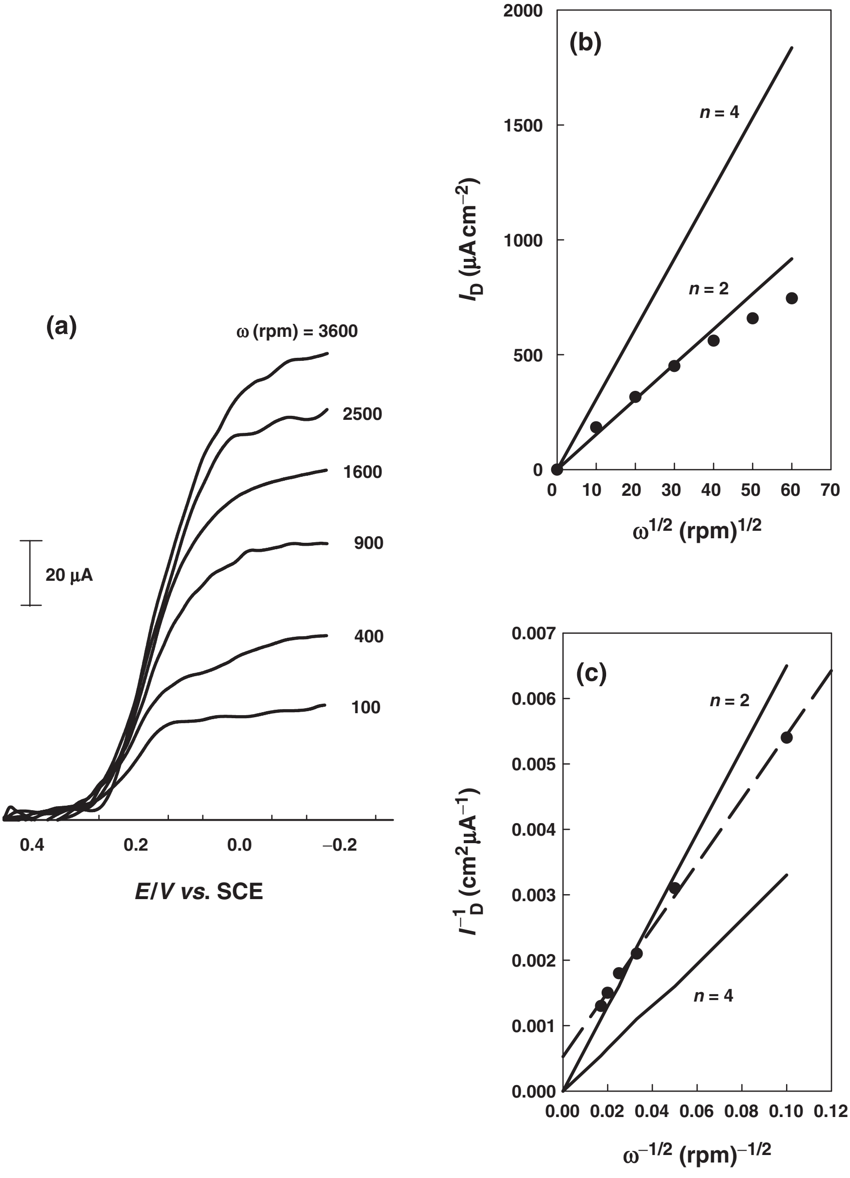

Figure 7. Reduction of O_2 at a rotating disk electrode coated with complex **4** after oxidation at 1.20 V. (a) Current–potential curves in air saturated 0.50 M $HClO_4$/0.25 M NH_4PF_6, scan rate = 5 mV s^{-1}. (b) Levich plot of plateau current *vs*. square root of the rotation rate for the curves in (a). (c) Koutecky–Levich plot of the inverse of the plateau current *vs*. the inverse of the square root of the rotation rate for the curves in (a). The theoretical two electron and four electron lines are marked $n = 2$ and $n = 4$, respectively

The results of the RDE experiments performed on an electrode coated with complex **4** and cycled anodically to 1.20 V prior to oxygen reduction are illustrated in figure 7(a). The Levich plot of the data, figure 7(b), shows similar deviations from linearity to those observed in figure 6(b) prior to anodic conditioning however the Koutecky–Levich plot of the experimental data falls between the theoretical $n = 2$ and $n = 4$ lines, figure 7(c).

The slope of this line reveals that approximately 50% of the oxygen is reduced to hydrogen peroxide and 50% is reduced to water. Studies are currently underway to determine if increasing the number of Pt(II) peripheral groups will result in 100% reduction of oxygen directly to water.

This study reports the synthesis of a new bimetallic cobalt(II)–platinum(II) porphyrin which shows enhanced catalytic abilities toward oxygen reduction when modified electrodes of the complex are anodically cycled in acidic media. This enhanced catalysis can in part be attributed to the dimethoxyphenyl substituents, which undergo electro-oxidation when anodically cycled in acidic media. Although platinum(II) does not directly interact with oxygen to cause enhanced catalysis it appears to play a role in the electro-reduction of oxygen as does cycling the coated electrode anodically. Formation of a new redox couple resulting from anodic cycling suggests formation of a new species on the electrode surface, which may create a more conductive film in intimate contact with the electrode surface.

Acknowledgements

The authors thank Research Corporation (Grant No. CC6074) and the University of Dayton start-up funds for their generous support of this research.

References

[1] P. Vasudevan, M. Neelam, S. Tyagi. *Trans. Met. Chem.*, **15**, 81 (1990).
[2] J.H. Zagal. *Coord. Chem. Rev.*, **119**, 89 (1992).
[3] A. Bettelheim, L. Soifer, E. Korin. *J. Electroanal. Chem.*, **571**, 265 (2004).
[4] A. Bettelheim, L. Soifer, E. Korin. *J. Power Source*, **130**, 158 (2004).
[5] C. Shi, F.C. Anson. *J. Am. Chem. Soc.*, **113**, 9564 (1991).
[6] J.P. Collman, L.L. Chng, D.A. Tyvoll. *Inorg. Chem.*, **34**, 1311 (1995).
[7] R.R. Durand Jr, C.S. Bencosme, J.P. Collman, F.C. Anson. *J. Am. Chem. Soc.*, **105**, 2710 (1983).
[8] C.J. Chang, Z.-H. Loh, C. Shi, F.C. Anson, D.B. Nocera. *J. Am. Chem. Soc.*, **126**, 10013 (2004).
[9] S. Fukuzumi, K. Okamoto, C.P. Gros, R. Guilard. *J. Am. Chem. Soc.*, **126**, 10441 (2004).
[10] F.C. Anson, C. Shi, B. Steiger. *Acc. Chem. Res.*, **30**, 437 (1997).
[11] J.E. Bennett, A. Burewicz, D.E. Wheeler, I. Eliezer, L. Czuchajowski, T. Malinski. *Inorg. Chim. Acta*, **271**, 167 (1998).
[12] T. Abe, M. Kaneko. *Prog. Poly. Sci.*, **28**, 1441 (2003).
[13] J. Qu, Y. Shen, X. Qu, S. Dong. *Electroanalysis*, **16**, 1444 (2004).
[14] S.M. Chen, Y.L. Chen. *J. Electroanal. Chem.*, **573**, 277 (2004).
[15] K. Araki, L. Angnes, C.M.N. Azevedo, H.E. Toma. *J. Electroanal. Chem.*, **397**, 205 (1995).
[16] J.M. Vago, V.C. Dall'Orto, E. Forzani, J. Hurst, I.N. Rezzano. *Sens. Act. B*, **96**, 407 (2003).
[17] G.E. Milczarek, A. Ciszewski. *Electroanalysis*, **13**, 164 (2001).
[18] H. Winnischofer, S.D. Lima, K. Araki, H.E. Toma. *Anal. Chim. Acta*, **480**, 97 (2003).
[19] A. Ciszewski, G. Milezarek. *Talanta*, **61**, 11 (2003).
[20] F. Armijo, M. Isaacs, G. Ramirez, E. Trollund, J. Canales, M.T. Aguirre. *J. Electroanal. Chem.*, **566**, 315 (2004).
[21] E.B. Fleischer, A.M. Schanchter. *Inorg. Chem.*, **30**, 3763 (1991).
[22] J.H. Price, A.N. Williamson, R.F. Schramm, B.B. Wayland. *Inorg. Chem.*, **11**, 1280 (1972).
[23] H. Yuan, L. Thomas, L.K. Woo. *Inorg. Chem.*, **35**, 2808 (1996).
[24] D. Marek, M. Narra, A. Schneider, S. Swavey. *Inorg. Chim. Acta*, **358**, 3430 (2005).
[25] A.D. Adler, F.R. Longo, F. Kampas, J. Kim. *J. Inorg. Nucl. Chem.*, **32**, 2443 (1970).
[26] K.M. Kadish, E.V. Caemelbecke. *J. Solid State Electrochem.*, **7**, 254 (2003).
[27] A.R. Brown, Z. Guo, F.W.J. Mosselmans, S. Parsons, M. Schröder, L.J. Yellowees. *J. Am. Chem. Soc.*, **120**, 8805 (1998).
[28] F.P. Fanizzi, G. Natile, M. Lanfranch, A. Tiripicchio, F. Laschi, P. Zanello. *Inorg. Chem.*, **35**, 3173 (1996).

[29] C. Arullo-McAdams, K.M. Kadish. *Inorg. Chem.*, **29**, 2749 (1990).
[30] J.S. Swenton. *Acc. Chem. Res.*, **16**, 74 (1983).
[31] D. Hawley, R.N. Adams. *J. Electroanal. Chem.*, **8**, 163 (1964).
[32] M. Michman, M. Oron. *Electrochim. Acta*, **39**, 2781 (1994).
[33] A.S. El-Tabl, K.Y. El-Baradic, R.M. Issa. *J. Coord. Chem.*, **56**, 1113 (2003).
[34] J. Koutecky, V.G. Levich. *Zh. Fiz. Khim.*, **32**, 1565 (1956).